Sensor and Simulation Notes

Note 569
(Revised)

April 2015

Examples of the Power Wave Theory of Antennas

Everett G. Farr
Farr Fields, LC
egfarr@gmail.com

Abstract

Power wave theory provides a complete and simple description of antenna performance in both the frequency and time domains. To clarify its usefulness, we provide here a number of examples. First, we show how the theory can be used to describe the performance of electrically small electric and magnetic dipoles; the so-called D-dot and B-dot sensors. We calculate the antenna transfer function, and then provide standard antenna parameters, including gain, realized gain, effective length, and effective area. Second, we show how a matching circuit can be combined with an antenna to form a combined Generalized Antenna Scattering Matrix. With this, we show how two common matching circuits affect antenna performance.

Note: This revision corrects minor errors that appeared in the original paper dated December 2014.

I. Introduction

In our papers on the power wave theory of antennas [1, 2], we showed a complete description of antenna performance in both the frequency and time domains. This fills a gap in current antenna theory by providing the simplest possible description of antenna performance in the time domain. It also fills a gap in the frequency domain, since neither antenna gain nor radar cross section include phase information.

Some reviewers of [1, 2] have requested examples of power waves applied to common antennas. We therefore provide here a series of examples that expand upon these ideas. First, we review the definitions of terms. Next, we show how the theory of power waves applies to electrically small electric and magnetic dipoles; or D-dot and B-dot sensors. Third, we show how to add a matching circuit to an antenna, and incorporate its scattering parameters into the Generalized Antenna Scattering Matrix. Finally, we show how some common matching circuits affect antenna performance.

We begin now with a review of the definitions.

II. Review of Power Waves as Applied to Antennas

We summarize here the power wave theory of antennas [1, 2]. In those two papers, we argued that an antenna can be reduced to a 3-port network. One port is the antenna port, and the second and third ports are the θ– and ϕ–polarizations of the incident and scattered fields. We define the following parameters relating to far-field performance as

$$
\begin{aligned}
\widetilde{\Pi}_{src} &= \frac{\widetilde{V}_{src}}{\sqrt{Z_{o1}}} && = \text{source power wave} \\
\widetilde{\Pi}_{rec} &= \frac{\widetilde{V}_{rec}}{\sqrt{Z_{o1}}} && = \text{received power wave} \\
\widetilde{\Sigma}_{\theta,inc} &= \frac{\widetilde{E}_{\theta,inc}}{\sqrt{Z_{o2}}} && = \text{incident power flux density wave, } \theta\text{ - component} \\
\widetilde{Y}_{\theta,rad} &= \frac{r\,\widetilde{E}_{\theta,rad}}{\sqrt{Z_{o2}}}e^{\gamma r} && = \text{radiated radiation intensity wave, } \theta\text{ - component} \\
\widetilde{\Sigma}_{\phi,inc} &= \frac{\widetilde{E}_{\phi,inc}}{\sqrt{Z_{o2}}} && = \text{incident power flux density wave, } \phi\text{ - component} \\
\widetilde{Y}_{\phi,rad} &= \frac{r\,\widetilde{E}_{\phi,rad}}{\sqrt{Z_{o2}}}e^{\gamma r} && = \text{radiated radiation intensity wave, } \phi\text{ - component}
\end{aligned}
\quad . \tag{2.1}
$$

Here, $\widetilde{E}_{rad}$ is the radiated far field, $\gamma = s/v = jk$, $s = j\omega$, and $k = \omega / v = 2\pi f / v$ is the propagation constant in the surrounding medium. Furthermore, v is the velocity of propagation in the surrounding medium, and r is the distance from the antenna to the observation point in the far field. In addition, Z_{o1} and Z_{o2} are the real reference impedances associated with the antenna port and the surrounding medium – most commonly, $Z_{o1} = 50\ \Omega$ and $Z_{o2} = 120\ \pi\Omega$. The tilde indicates that we are operating in the Laplace domain.

The symbols Π, Y, and Σ are Greek versions of P, U, and S, which are the commonly used symbols for power, radiation intensity, and power flux density, respectively. Thus, to convert the symbol for a "power" quantity to that of a "power wave" quantity, we make the symbol Greek.

The above quantities are assembled into the antenna equation, which is a 3x3 matrix equation. We can express these two different ways, leading to

$$
\begin{bmatrix} \tilde{b}_1 \\ \tilde{b}_2 \\ \tilde{b}_3 \end{bmatrix} = \begin{bmatrix} \tilde{S}_{11} & \tilde{S}_{12} & \tilde{S}_{13} \\ \tilde{S}_{21} & \tilde{S}_{22} & \tilde{S}_{23} \\ \tilde{S}_{31} & \tilde{S}_{32} & \tilde{S}_{33} \end{bmatrix} \begin{bmatrix} \tilde{a}_1 \\ \tilde{a}_2 \\ \tilde{a}_3 \end{bmatrix}
$$

$$
\begin{bmatrix} \tilde{\Pi}_{rec}(\theta',\phi') \\ \tilde{Y}_{\theta,rad}(\theta,\phi,\theta',\phi') \\ \tilde{Y}_{\phi,rad}(\theta,\phi,\theta',\phi') \end{bmatrix} = \begin{bmatrix} \tilde{\Gamma} & \tilde{h}_\theta(\theta',\phi') & \tilde{h}_\phi(\theta',\phi') \\ s\,\tilde{h}_\theta(\theta,\phi)/(2\pi v) & \tilde{\ell}_{\theta\theta}(\theta,\phi,\theta',\phi') & \tilde{\ell}_{\theta\phi}(\theta,\phi,\theta',\phi') \\ s\,\tilde{h}_\phi(\theta,\phi)/(2\pi v) & \tilde{\ell}_{\phi\theta}(\theta,\phi,\theta',\phi') & \tilde{\ell}_{\phi\phi}(\theta,\phi,\theta',\phi') \end{bmatrix} \begin{bmatrix} \tilde{\Pi}_{src} \\ \tilde{\Sigma}_{\theta,inc}(\theta',\phi') \\ \tilde{\Sigma}_{\theta,inc}(\theta',\phi') \end{bmatrix}, \tag{2.2}
$$

where $\tilde{\Gamma}$ is the reflection coefficient looking into the antenna port, the two components of $\tilde{h}$ represent the vector transfer function, and the four components of $\tilde{\ell}$ represent the dyadic scattering coefficient. The unprimed angular coordinates are the angles of observation, and the primed coordinates are the angles of incidence.

From the transfer function one can calculate antenna gain, realized gain, effective area, and effective length. From the scattering coefficient one can calculate radar cross section or scattering cross section of the antenna.

A signal flow graph of this equation is shown in Figure 2.1. We will add a matching circuit to this in Section IV.

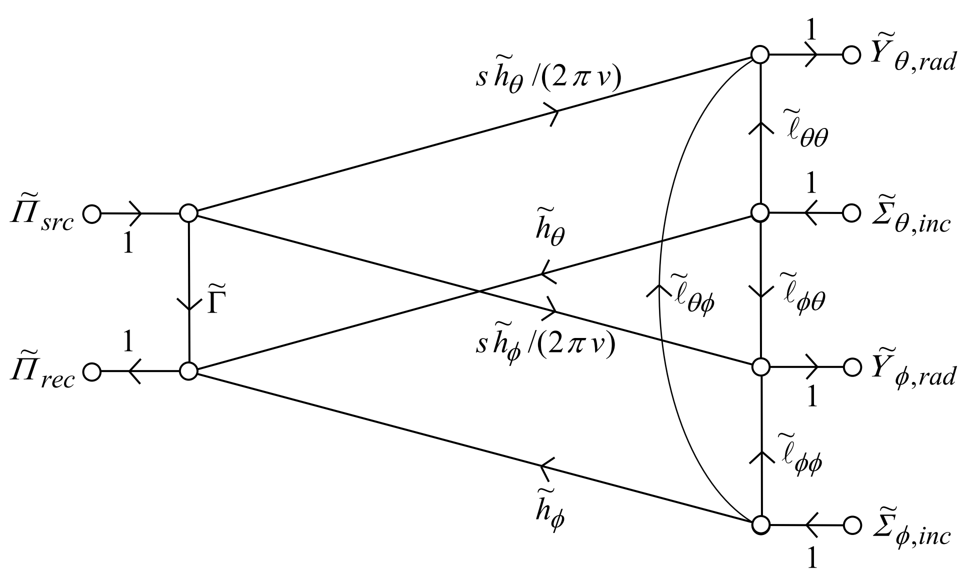

Figure 2.1. Signal flow graph of the antenna equation.

III. D-dot and B-dot Antennas

For our first examples, we calculate the various antenna parameters of D-dot and B-dot sensors.

A. D-dot Sensor

We begin with the D-dot sensor, which is an electrically small electric dipole driving a resistive load of Z_{o1}. The received voltage across the load in both the time and frequency domains is [3, p. 86]

$$\begin{aligned} \tilde{V}_{rec} &= A_{eq}\, Z_{o1}\, s\, \tilde{D}_{inc} = \varepsilon\, A_{eq}\, Z_{o1}\, s\, \tilde{E}_{inc} \\ V_{rec}(t) &= \varepsilon\, A_{eq}\, Z_{o1} \frac{d\, E_{inc}(t)}{dt} \end{aligned} \quad , \tag{3.1}$$

where ε is the permittivity of the surrounding medium. We are restricting the treatment for now to dominant polarization at an angle of maximum coupling. We generalize to an arbitrary angle of incidence at the end of this subsection. The expression for antenna transfer function and impulse response are obtained from [1, 2, eqns. (2.11) and (2.15)] as

$$\begin{aligned} \frac{\tilde{V}_{rec}}{\sqrt{Z_{o1}}} &= \tilde{h}\, \frac{\tilde{E}_{inc}}{\sqrt{Z_{o2}}} \\ \frac{V_{rec}(t)}{\sqrt{Z_{o1}}} &= h(t) \ * \ \frac{E_{inc}(t)}{\sqrt{Z_{o2}}} \end{aligned} \quad , \tag{3.2}$$

where " * " is the convolution operator and Z_{o2} is the impedance of the surrounding medium. The surrounding medium is normally free space, for which $Z_{o2} = 120\,\pi\,\Omega$. Comparing eqns. (3.1) and (3.2), we find the transfer function and impulse response of the D-dot sensor as

$$\begin{aligned} \tilde{h} &= \varepsilon\, A_{eq} \sqrt{Z_{o1} Z_{o2}}\, s &&= \frac{A_{eq}}{v} \sqrt{\frac{Z_{o1}}{Z_{o2}}}\, s \\ h(t) &= \varepsilon\, A_{eq} \sqrt{Z_{o1} Z_{o2}}\, \delta'(t) &&= \frac{A_{eq}}{v} \sqrt{\frac{Z_{o1}}{Z_{o2}}}\, \delta'(t) \end{aligned} \quad , \tag{3.3}$$

where $\delta'(t)$ is the time derivative of the Dirac delta function, and we have used $\varepsilon = 1/(Z_{o2}\, v)$. Looking into the port, the input impedance looks like a capacitor of value C. The reflection coefficient looking into the port is therefore

$$\tilde{\Gamma} = \frac{1/(sC) - Z_{o1}}{1/(sC) + Z_{o1}} = \frac{1 - s\tau_e}{1 + s\tau_e} \quad , \qquad \tau_e = Z_{o1} C \quad . \tag{3.4}$$

With these parameters defined, we can now calculate all the common antenna parameters listed in Section IV of [1, 2]. From eqn. (4.4) of [1, 2], realized gain is

$$G_r(s) = \frac{4\pi}{\lambda^2}|\tilde{h}|^2 = \frac{4\pi}{\lambda^2}\frac{A_{eq}^{\;2}}{v^2}\frac{Z_{o1}}{Z_{o2}}|s|^2 \quad . \tag{3.5}$$

For the usual case where $s = j2\pi f$, and noting that $f = v/\lambda$, this simplifies to

$$G_r(f) = 16\pi^3 A_{eq}^{\;2}\frac{Z_{o1}}{Z_{o2}}\frac{f^4}{v^4} = 16\pi^3 A_{eq}^{\;2}\frac{Z_{o1}}{Z_{o2}}\frac{1}{\lambda^4} \quad . \tag{3.6}$$

Next, gain can be found from eqn. (4.8) in [1, 2],

$$G(s) = \frac{G_r(s)}{1-\left|\tilde{\Gamma}\right|^2} \quad . \tag{3.7}$$

The effective length is calculated from eqn. (4.11) in [1, 2] as

$$\begin{aligned} \tilde{h}_V &= \frac{\tilde{Z}_{in} + Z_{o1}}{Z_{o1}}\sqrt{\frac{Z_{o1}}{Z_{o2}}}\,\tilde{h} = \frac{1/(sC) + Z_{o1}}{Z_{o1}}\sqrt{\frac{Z_{o1}}{Z_{o2}}}\frac{A_{eq}}{v}\sqrt{\frac{Z_{o1}}{Z_{o2}}}\,s \\ &= \frac{1+s\tau_e}{s\tau_e}\frac{Z_{o1}}{Z_{o2}}\frac{A_{eq}}{v}\,s \end{aligned} \quad . \tag{3.8}$$

The effective area of the D-dot sensor is now calculated from eqn. (4.14) of [1, 2] as

$$\begin{aligned} A_e(s) &= \frac{\left|\tilde{h}\right|^2}{1-\left|\tilde{\Gamma}\right|^2} = \frac{1}{1-\left|\tilde{\Gamma}\right|^2}\frac{A_{eq}^{\;2}}{v^2}\frac{Z_{o1}}{Z_{o2}}|s|^2 \\ A_e(f) &= \frac{4\pi^2 A_{eq}^{\;2}}{1-\left|\tilde{\Gamma}\right|^2}\frac{Z_{o1}}{Z_{o2}}\frac{f^2}{v^2} = \frac{4\pi^2 A_{eq}^{\;2}}{1-\left|\tilde{\Gamma}\right|^2}\frac{Z_{o1}}{Z_{o2}}\frac{1}{\lambda^2} \end{aligned} \quad . \tag{3.9}$$

This completes the calculation of the various parameters of a D-dot sensor.

Note that eqn. (3.9) contains both effective area, A_e, and equivalent area, A_{eq}. It should be clear that these are two very different quantities that both just happen to have dimensions of meters squared.

To generalize the above to arbitrary angles of incidence, one multiplies the transfer function and impulse response by $\cos(\theta)$, where θ is the angle between the angle of incidence and the angle of maximum coupling. One would then modify the subsequent formulas accordingly.

B. B-dot Sensor

Next, we consider a B-dot sensor, or electrically small magnetic dipole driving a resistive load of Z_{o1}. The received voltage across the load in both the time and frequency domains is [3, p. 94]

$$\begin{aligned} \tilde{V}_{rec} &= A_{eq}\, s\, \tilde{B}_{inc} = \frac{s\, A_{eq}}{v}\, \tilde{E}_{inc} \\ V_{rec}(t) &= \frac{A_{eq}}{v}\, \frac{d\, E_{inc}(t)}{dt} \end{aligned} \quad , \tag{3.10}$$

where we have used $\tilde{B}_{inc} = \tilde{E}_{inc} / v$. As before, this treatment is for dominant polarization at an angle of maximum coupling. Compare this now to eqn. (3.2), and we get

$$\begin{aligned} \tilde{h} &= \frac{A_{eq}}{v} \sqrt{\frac{Z_{o2}}{Z_{o1}}}\, s \\ h(t) &= \frac{A_{eq}}{v} \sqrt{\frac{Z_{o2}}{Z_{o1}}}\, \delta'(t) \end{aligned} \quad . \tag{3.11}$$

Note the similarity to eqn. (3.3). Looking into the port, the input impedance looks like an inductor of value L. The reflection coefficient looking into the sensor from the port is

$$\tilde{\Gamma} = \frac{sL - Z_{o1}}{sL + Z_{o1}} = \frac{s\tau_m - 1}{s\tau_m + 1} \quad , \qquad \tau_m = L / Z_{o1} \quad . \tag{3.12}$$

The antenna parameters are calculated as before. Thus, realized gain and gain are

$$\begin{aligned} G_r(s) &= \frac{4\pi}{\lambda^2} |\, \tilde{h}\, |^2 = \frac{4\pi}{\lambda^2} \frac{{A_{eq}}^2}{v^2} \frac{Z_{o2}}{Z_{o1}} |s|^2 \\ G_r(f) &= 16\pi^3\, {A_{eq}}^2\, \frac{Z_{o2}}{Z_{o1}} \frac{f^4}{v^4} = 16\pi^3\, {A_{eq}}^2\, \frac{Z_{o2}}{Z_{o1}} \frac{1}{\lambda^4} \\ G(s) &= \frac{G_r(s)}{1 - \left|\tilde{\Gamma}\right|^2} \end{aligned} \quad . \tag{3.13}$$

The effective length is calculated from [1, 2, eqn. (4.11)] as

$$\begin{aligned} \tilde{h}_V &= \frac{\tilde{Z}_{in} + Z_{o1}}{Z_{o1}} \sqrt{\frac{Z_{o1}}{Z_{o2}}}\, \tilde{h} = \frac{sL + Z_{o1}}{Z_{o1}} \sqrt{\frac{Z_{o1}}{Z_{o2}}} \frac{A_{eq}}{v} \sqrt{\frac{Z_{o2}}{Z_{o1}}}\, s \\ &= (s\tau_m + 1) \frac{A_{eq}}{v}\, s \end{aligned} \quad . \tag{3.14}$$

The effective area of the B-dot sensor is now calculated as before from (4.14), leading to

$$\begin{aligned} A_e(s) &= \frac{\left|\tilde{h}\right|^2}{1-\left|\tilde{\Gamma}\right|^2} = \frac{1}{1-\left|\tilde{\Gamma}\right|^2} \frac{A_{eq}{}^2}{v^2} \frac{Z_{o2}}{Z_{o1}} |s|^2 \\ A_e(f) &= \frac{4\pi^2 A_{eq}{}^2}{1-\left|\tilde{\Gamma}\right|^2} \frac{Z_{o2}}{Z_{o1}} \frac{f^2}{v^2} = \frac{4\pi^2 A_{eq}{}^2}{1-\left|\tilde{\Gamma}\right|^2} \frac{Z_{o2}}{Z_{o1}} \frac{1}{\lambda^2} \end{aligned} \quad . \tag{3.15}$$

This completes the calculation of the various parameters of a B-dot sensor. One can modify this for off-boresight incidence as we did for the D-dot sensor, above.

IV. Adding a Matching Circuit to an Antenna

Next, we modify the Generalized Antenna Scattering Matrix to include a matching circuit. The antenna is still described by a 3x3 matrix, but it becomes more complicated due to the presence of the matching circuit.

We begin with a signal flow graph of the antenna, slightly modified from Figure 2.1, shown in Figure 4.1. The subscript *a* indicates that these are S-parameters of the antenna. Recall that these S-parameters are not unitless, as would normally be the case.

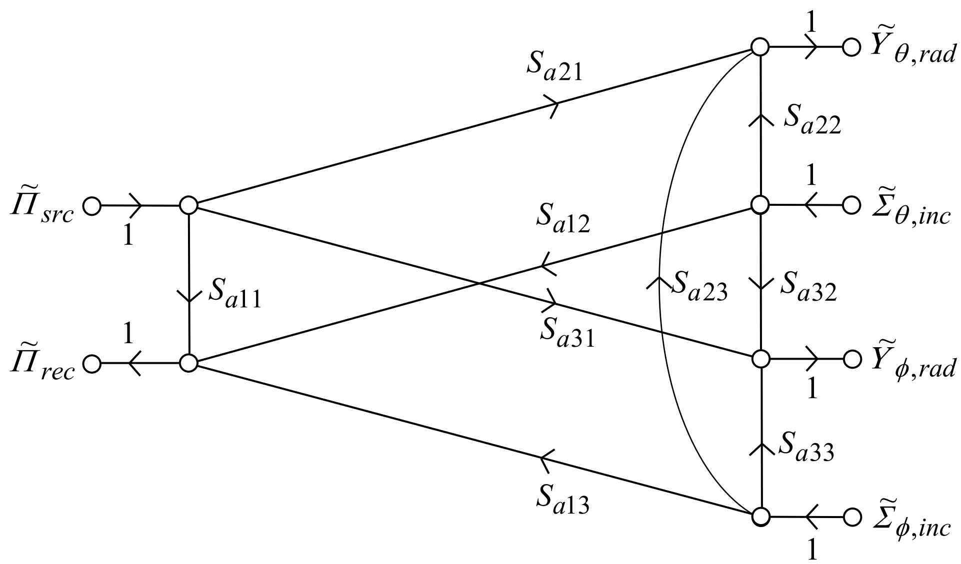

Figure 4.1. Signal flow graph of the antenna with a matching circuit added.

The matching circuit is expressed in terms of S-parameters, and its signal flow graph is shown in Figure 4.2. The subscript *m* indicates that these are parameters of the matching circuit. Note that the two real reference impedances, Z_{mo1} and Z_{mo2}, may be different, which is consistent with the theory of generalized S-parameters. The only constraint is that the reference impedance at port 2 of the matching network must match the reference impedance at the input port of the antenna.

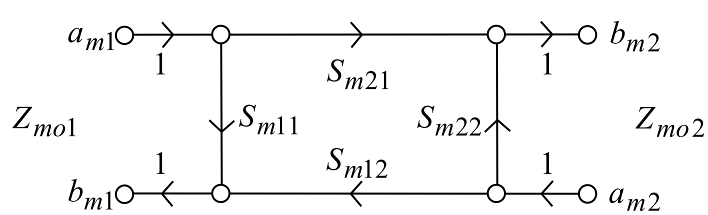

Figure 4.2 Signal flow graph of the matching circuit.

We now cascade the above two signal flow graphs to get the signal flow graph of the combined circuit, shown in Figure 4.3.

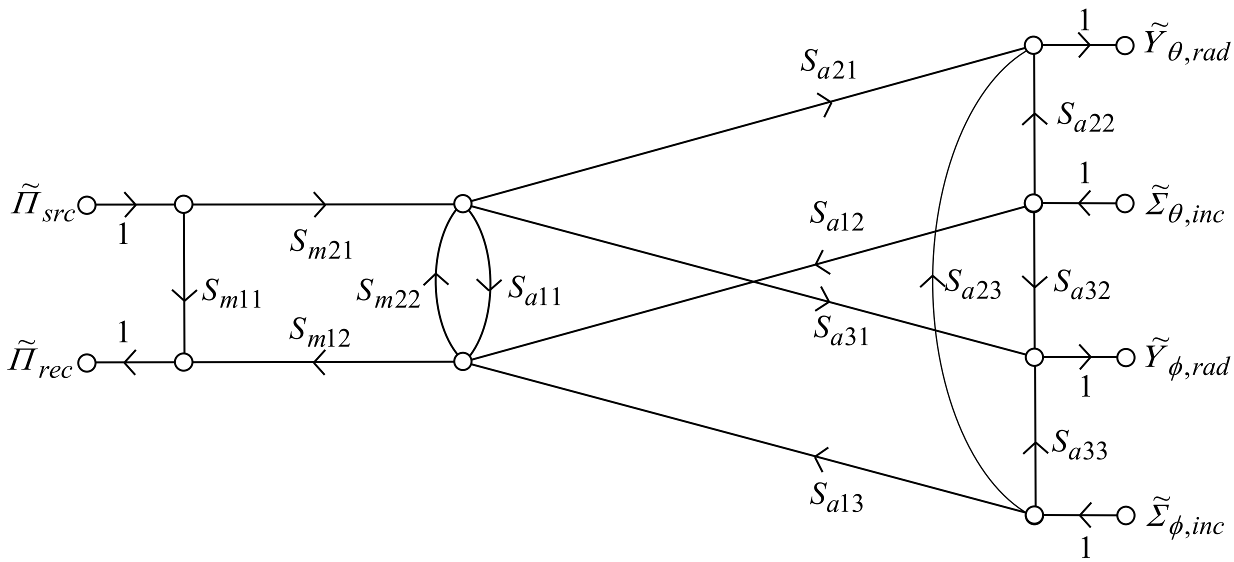

Figure 4.3. Signal flow graph of the antenna with a matching circuit added.

We now have to simplify this to a standard 3x3 matrix of the form

$$\begin{bmatrix} \widetilde{\Pi}_{rec} \\ \widetilde{Y}_{\theta,rad} \\ \widetilde{Y}_{\phi,rad} \end{bmatrix} = \begin{bmatrix} S_{c11} & S_{c12} & S_{c13} \\ S_{c21} & S_{c22} & S_{c23} \\ S_{c31} & S_{c32} & S_{c33} \end{bmatrix} \begin{bmatrix} \widetilde{\Pi}_{src} \\ \widetilde{\Sigma}_{\theta,inc} \\ \widetilde{\Sigma}_{\theta,inc} \end{bmatrix}, \tag{4.1}$$

where the subscript *c* refers to the combined antenna and matching network. A signal flow graph of this equation is shown in Figure 4.4.

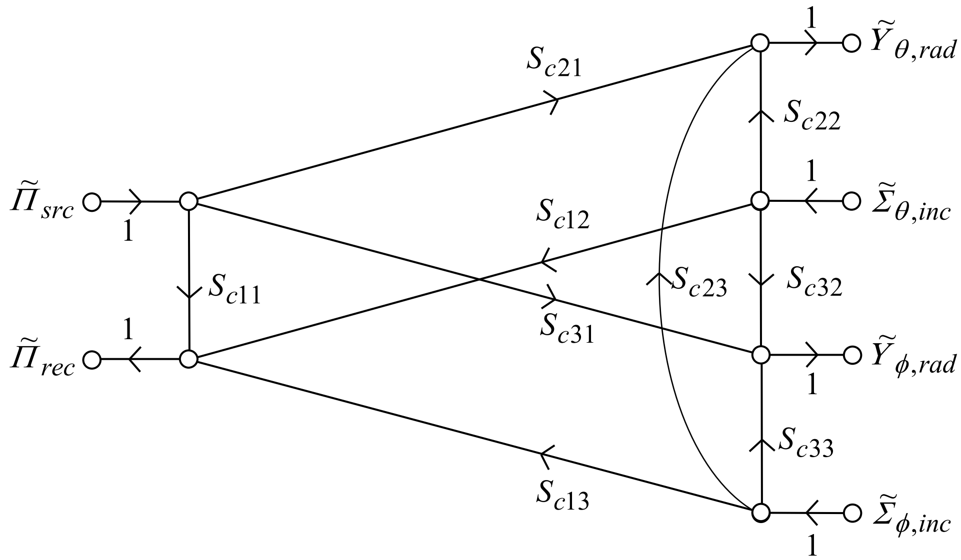

Figure 4.4. Signal flow graph of the antenna with a matching circuit added.

To implement the simplification, one has to solve for each of the nine elements of the combined S-parameter matrix, S_{cij}., each of which is the ratio of one of the three outputs to one of the three inputs. This is most simply done by using the 4 rules for simplifying signal flow graphs [4, p. 215], although Mason's rule works as well.

While it is unnecessary to show the details of the solution for all nine matrix elements, it will be useful to show a couple of examples. We begin by solving for S_{c11}. To begin the process, we eliminate the portions of Figure 4.3 that are not relevant, and show the result in Figure 4.5.

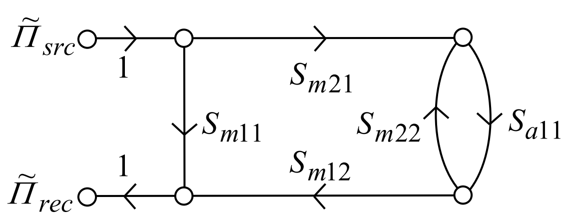

Figure 4.5. Signal flow graph simplified to calculate S_{c11}.

We now solve this using the four rules. The result is

$$\begin{aligned} S_{c11} &= \frac{\widetilde{\Pi}_{rec}}{\widetilde{\Pi}_{src}} = S_{m11} + \frac{S_{m21}\,S_{a11}\,S_{m12}}{\Delta} \quad . \\ \Delta &= 1 - S_{a11} S_{m22} \end{aligned} \tag{4.2}$$

Similarly, we solve for S_{c21}. As before, we eliminate the unnecessary parts of Figure 4.3 to obtain the simplified version shown in Figure 4.6.

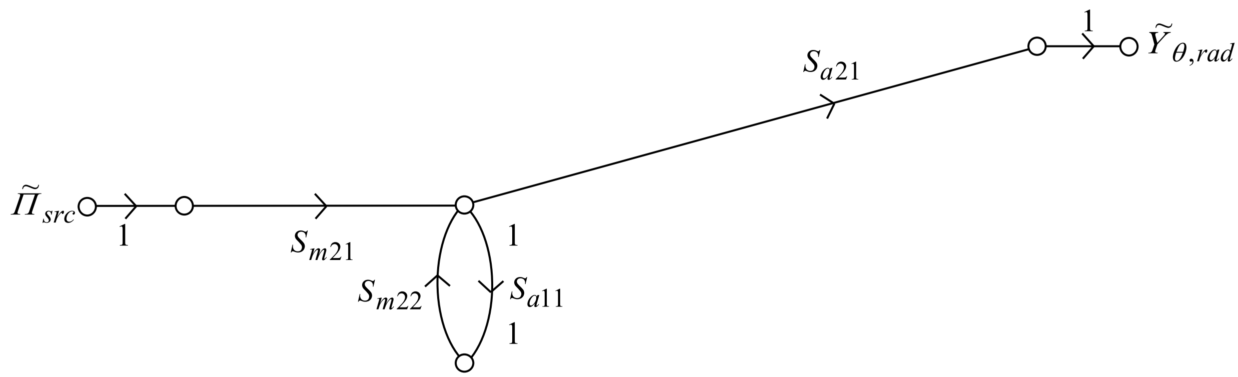

Figure 4.6. Signal flow graph simplified to calculate S_{c21}.

The four rules allow one to simplify this to

$$\begin{aligned} S_{c21} &= \frac{\tilde{Y}_{\theta,rad}}{\tilde{\Pi}_{src}} = \frac{S_{m21}S_{a21}}{\Delta} \quad . \\ \Delta &= 1 - S_{a11}S_{m22} \end{aligned} \tag{4.3}$$

The process continues for all nine elements. The final result is

$$\begin{bmatrix} \tilde{\Pi}_{rec} \\ \tilde{Y}_{\theta,rad} \\ \tilde{Y}_{\phi,rad} \end{bmatrix} = \begin{bmatrix} S_{m11} + \dfrac{S_{m21}S_{a11}S_{m12}}{\Delta} & \dfrac{S_{a12}S_{m12}}{\Delta} & \dfrac{S_{a13}S_{m12}}{\Delta} \\ \dfrac{S_{m21}S_{a21}}{\Delta} & S_{a22} + \dfrac{S_{a12}S_{m22}S_{a21}}{\Delta} & S_{a23} + \dfrac{S_{a13}S_{m22}S_{a21}}{\Delta} \\ \dfrac{S_{m21}S_{a31}}{\Delta} & S_{a32} + \dfrac{S_{a12}S_{m22}S_{a31}}{\Delta} & S_{a33} + \dfrac{S_{a13}S_{m22}S_{a31}}{\Delta} \end{bmatrix} \begin{bmatrix} \tilde{\Pi}_{src} \\ \tilde{\Sigma}_{\theta,inc} \\ \tilde{\Sigma}_{\theta,inc} \end{bmatrix}$$

$$\Delta = 1 - S_{a11}S_{m22} \tag{4.4}$$

This is a Generalized Antenna Scattering Matrix that includes the effects of a matching circuit. By using eqn (2.2), this may alternatively be expressed as

$$\begin{bmatrix} \widetilde{\Pi}_{rec} \\ \widetilde{Y}_{\theta,rad} \\ \widetilde{Y}_{\phi,rad} \end{bmatrix} = \begin{bmatrix} S_{m11} + \dfrac{S_{m21} S_{m12} \widetilde{\Gamma}}{\Delta} & \dfrac{S_{m12}\, \widetilde{h}_\theta}{\Delta} & \dfrac{S_{m12} \widetilde{h}_\phi}{\Delta} \\ \dfrac{s\, S_{m21}\, \widetilde{h}_\theta}{2\,\pi\, v\, \Delta} & \widetilde{\ell}_{\theta\theta} + \dfrac{s\, S_{m22}\, \widetilde{h}_\theta{}^2}{2\,\pi\, v\, \Delta} & \widetilde{\ell}_{\theta\phi} + \dfrac{s\, S_{m22}\, \widetilde{h}_\theta \widetilde{h}_\phi}{2\,\pi\, v\, \Delta} \\ \dfrac{s\, S_{m21}\, \widetilde{h}_\phi}{2\,\pi\, v\, \Delta} & \widetilde{\ell}_{\phi\theta} + \dfrac{s\, S_{m22}\, \widetilde{h}_\phi \widetilde{h}_\theta}{2\,\pi\, v\, \Delta} & \widetilde{\ell}_{\phi\phi} + \dfrac{s\, S_{m22}\, \widetilde{h}_\phi{}^2}{2\,\pi\, v\, \Delta} \end{bmatrix} \begin{bmatrix} \widetilde{\Pi}_{src} \\ \widetilde{\Sigma}_{\theta,inc} \\ \widetilde{\Sigma}_{\theta,inc} \end{bmatrix} .$$

$$\Delta = 1 - S_{m22}\, \widetilde{\Gamma} \tag{4.5}$$

Note that $S_{c32} = S_{c23}$, since $\widetilde{\ell}_{\theta\phi} = \widetilde{\ell}_{\phi\theta}$.

In the following section we consider some examples.

V. Some Common Matching Circuits

We consider here the effects of two common matching circuits on antennas.

A. IRA Splitter Balun

A balun commonly used with Impulse Radiating Antennas is the so-called splitter balun. It consists of two equal lengths of 100 Ω cable connected in parallel at the input port and in series at the output port. This implements a wideband lossless impedance transition from 50 Ω to 200 Ω, which is a common input impedance for an IRA.

A sketch of the balun is shown in Figure 5.1. Note the different reference impedances at the two ports, 50 Ω on the left, and 200 Ω on the right.

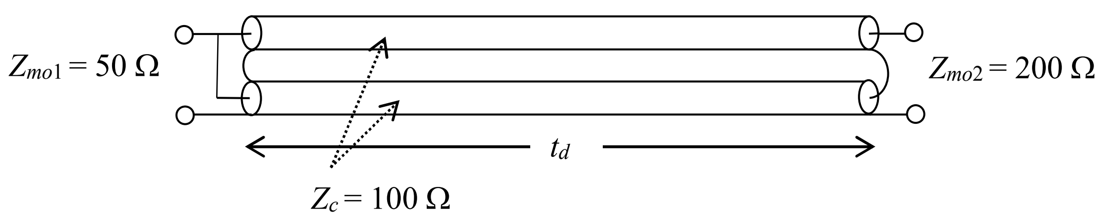

Figure 5.1. Sketch of the IRA splitter balun.

The scattering parameters of an ideal splitter balun are

$$\begin{aligned} \begin{bmatrix} b_{m1} \\ b_{m2} \end{bmatrix} &= \begin{bmatrix} S_{m11} & S_{m12} \\ S_{m21} & S_{m22} \end{bmatrix} \begin{bmatrix} a_{m1} \\ a_{m2} \end{bmatrix} \\ \begin{bmatrix} b_{m1} \\ b_{m2} \end{bmatrix} &= \begin{bmatrix} 0 & e^{-st_d} \\ e^{-st_d} & 0 \end{bmatrix} \begin{bmatrix} a_{m1} \\ a_{m2} \end{bmatrix} \end{aligned} , \tag{5.1}$$

where t_d is the time delay of the two cable lengths. The signal flow graph of this is shown in Figure 5.2

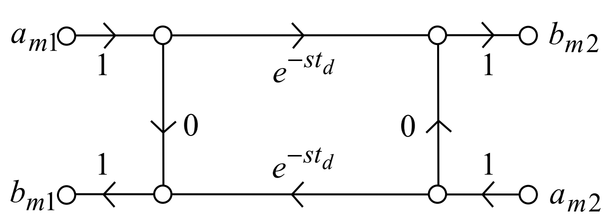

Figure 5.2. Signal flow graph of the IRA splitter balun.

We can now substitute these values into equation (4.4) to get the combined response of the antenna and matching circuit

$$\begin{bmatrix} \tilde{\Pi}_{rec} \\ \tilde{Y}_{\theta,rad} \\ \tilde{Y}_{\phi,rad} \end{bmatrix} = \begin{bmatrix} e^{-2st_d} S_{a11} & e^{-st_d} S_{a12} & e^{-st_d} S_{a13} \\ e^{-st_d} S_{a21} & S_{a22} & S_{a23} \\ e^{-st_d} S_{a31} & S_{a32} & S_{a33} \end{bmatrix} \begin{bmatrix} \tilde{\Pi}_{src} \\ \tilde{\Sigma}_{\theta,inc} \\ \tilde{\Sigma}_{\theta,inc} \end{bmatrix} \quad . \tag{5.2}$$

So the only effect of an ideal splitter balun is to add some time delays to the antenna response. But it realizes the useful function of stepping up the impedance from 50 Ω to 200 Ω over a broad bandwidth.

B. Quarter Wave Transformer

Another way to implement an impedance match is to use a quarter-wave transformer. This time, the impedance match works only at a specific frequency, $s_o = j\,2\,\pi f_o$, where $f_o = v_c / \lambda_o$, v_c is the velocity of propagation in the cable, and λ_o is the wavelength in the cable at the operating frequency. Thus, the cable length is

$$\ell = \frac{\lambda_o}{4} = \frac{v_c}{4\,f_o} \quad . \tag{5.3}$$

The cable impedance is chosen so that

$$Z_c = \sqrt{Z_{mo1}\, Z_{mo2}} \quad , \tag{5.4}$$

where Z_{mo1} and Z_{mo2} are the impedances at the input and output, respectively. A sketch of the quarter wave transformer is shown in Figure 5.3. Note once again that the reference impedances are different at each end.

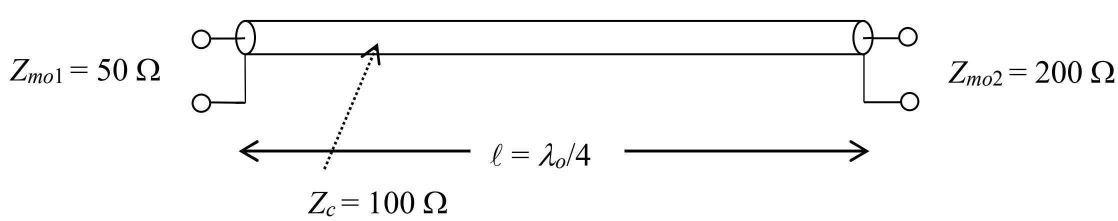

Figure 5.3. A quarter wave transformer.

At the operating frequency, the scattering parameters of the quarter-wave transformer are

$$
\begin{aligned}
\begin{bmatrix} b_{m1} \\ b_{m2} \end{bmatrix} &= \begin{bmatrix} S_{m11} & S_{m12} \\ S_{m21} & S_{m22} \end{bmatrix} \begin{bmatrix} a_{m1} \\ a_{m2} \end{bmatrix} \\
\begin{bmatrix} b_{m1} \\ b_{m2} \end{bmatrix} &= \begin{bmatrix} 0 & -j \\ -j & 0 \end{bmatrix} \begin{bmatrix} a_{m1} \\ a_{m2} \end{bmatrix}
\end{aligned} \quad . \tag{5.5}
$$

The signal flow graph at the operating frequency is shown in Figure 5.4

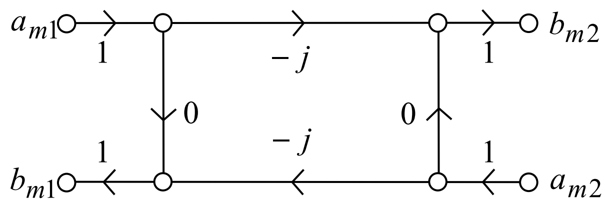

Figure 5.4. Signal flow graph of a quarter-wave transformer at the operating frequency.

We can now substitute these values into eqn. (4.4) to get the combined response of the antenna and matching circuit

$$
\begin{bmatrix} \tilde{\Pi}_{rec} \\ \tilde{Y}_{\theta,rad} \\ \tilde{Y}_{\phi,rad} \end{bmatrix} = \begin{bmatrix} -S_{a11} & -j\,S_{a12} & -j\,S_{a13} \\ -j\,S_{a21} & S_{a22} & S_{a23} \\ -j\,S_{a31} & S_{a32} & S_{a33} \end{bmatrix} \begin{bmatrix} \tilde{\Pi}_{src} \\ \tilde{\Sigma}_{\theta,inc} \\ \tilde{\Sigma}_{\theta,inc} \end{bmatrix} \quad . \tag{5.6}
$$

Thus, at its operating frequency, the quarter wave transformer has little effect on antenna performance, except to add some phase shifts to some of the factors in the GASM. But it realizes the useful effect of stepping up the impedance, in this case from 50 Ω to 200 Ω, at a single operating frequency.

VI. Conclusions

We have provided here a few examples of how the theory of power waves clarifies antenna performance. We have shown how to calculate the transfer function and impulse response of D-dot and B-dot sensors. This led to calculations of the gain, realized gain, effective length, and effective area of the sensors. We have also shown how to add a matching circuit to the Generalized Antenna Scattering Matrix. We used these results to show the effects of adding a splitter balun and a quarter-wave transformer to the front end of an antenna. While these examples were solved in the frequency domain, their conversion to the time domain is straightforward.

This set of examples demonstrates the usefulness and flexibility of the power wave theory. We believe that this is the simplest and most complete description of antenna performance in both the time and frequency domains. So we encourage the antenna community to add the various terms associated with power wave theory to the next revision of the antenna definitions standards [5].

Acknowledgments

I am grateful to the anonymous reviewers of my last paper, who suggested the sample problems solved here.

References

Note that Sensor and Simulation Notes are available from the Summa Foundation web site, www.ece.unm.edu/summa/notes/

1. E. G. Farr, "A Power Wave Theory of Antennas, Fourth Revision" Sensor and Simulation Note 564, December 2014.

2. E. G. Farr, "A Power Wave Theory of Antennas," published in FERMAT e-magazine, www.e-fermat.org, Vol. 7, 2015.

3. C. E. Baum, "Electromagnetic Sensors and Meausurement Techniques," pp. 73-144 in J. E. Thompson and L. H. Lewison (editors), *Fast Electrical and Optical Measurements,* Martinus Nijhoff Publishers, Dordrecht, 1986.

4. D. M. Pozar, *Microwave Engineering*, Second Edition, New York, John Wiley & Sons, 1998.

5. IEEE, *IEEE Standard Definitions of Terms for Antennas*, IEEE Std. 145-1993, Institute for Electrical and Electronics Engineering, Inc., New York, March 1993.